

The background features two complex, chaotic trajectories. On the left, a dense, tangled path of green lines forms a circular, swirling pattern. On the right, a blue trajectory starts as a single line and branches out into a complex, multi-lobed structure, resembling a butterfly or a complex orbit. The overall aesthetic is scientific and mathematical, set against a dark background.

STATE ESTIMATION OF CHAOTIC TRAJECTORIES: A HIGHER-DIMENSIONAL, GRID-BASED, BAYESIAN APPROACH TO UNCERTAINTY PROPAGATION

Benjamin L. Hanson

Ph.D. student, Jacobs School of Engineering

Department of Mechanical and Aerospace Engineering

UC San Diego, La Jolla, CA

blhanson@ucsd.edu

2024 AIAA/AAS Space Flight Mechanics Meeting

Monday 8 January 2024

A Look Back at the History of Orbital State Estimation...



1969



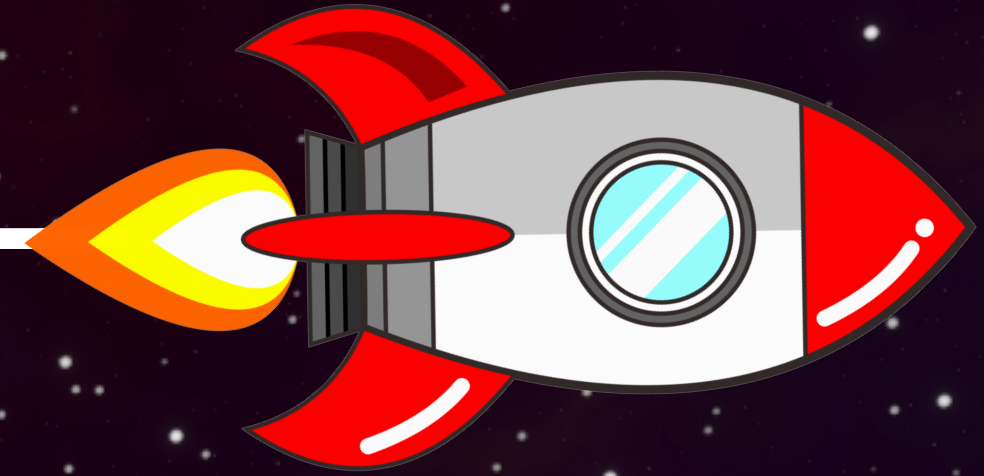
1981



1996



2022



...All Utilized the
Extended Kalman Filter!

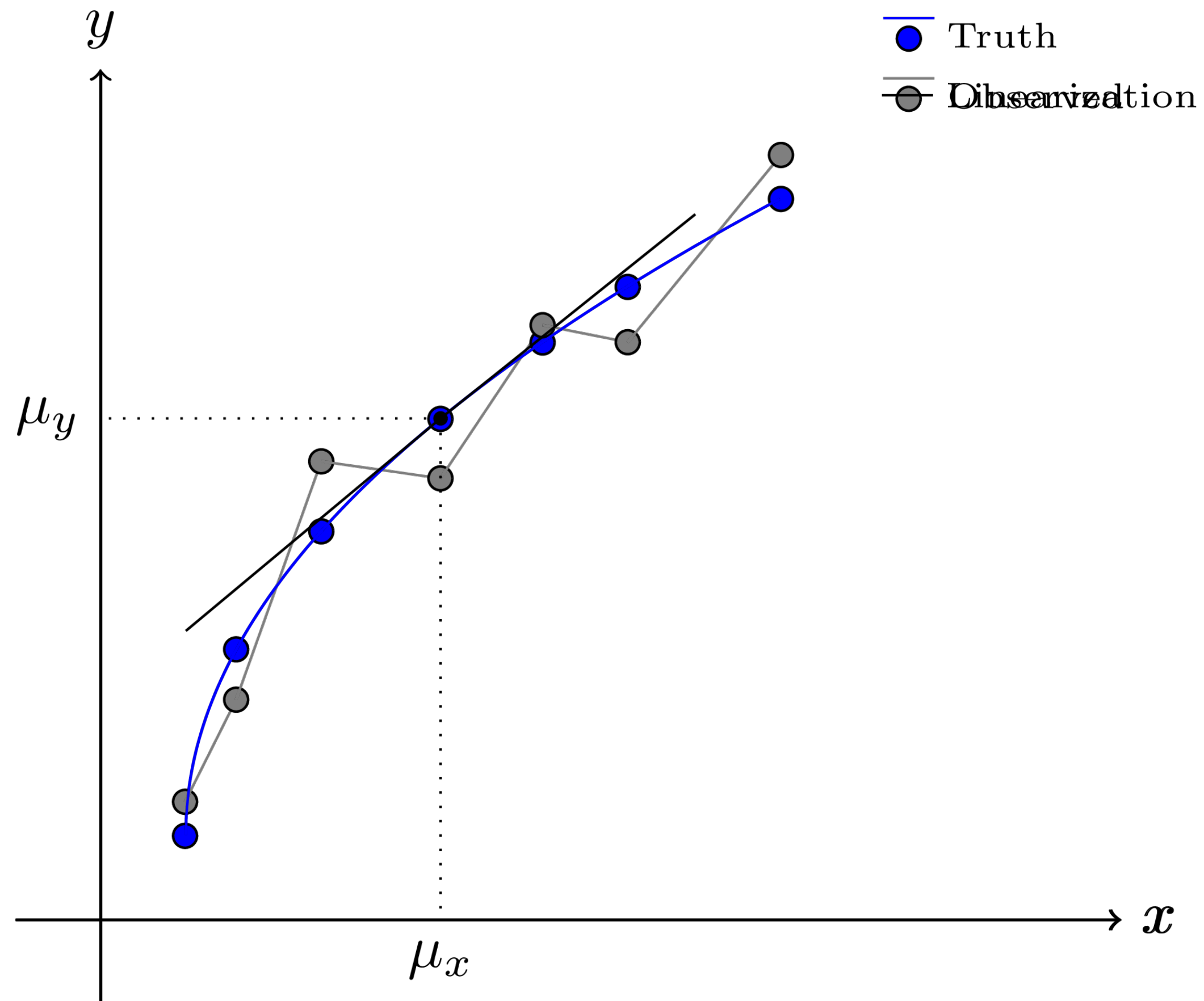


The Extended Kalman Filter

Assumptions and Limitations



- EKF linearizes the nonlinear system about an estimate mean value, assuming that the observations are frequent enough that the linearization is accurate



Model: $\dot{\mathbf{x}} = \mathbf{f}(\mathbf{x}, t) + \mathbf{w}(t)$

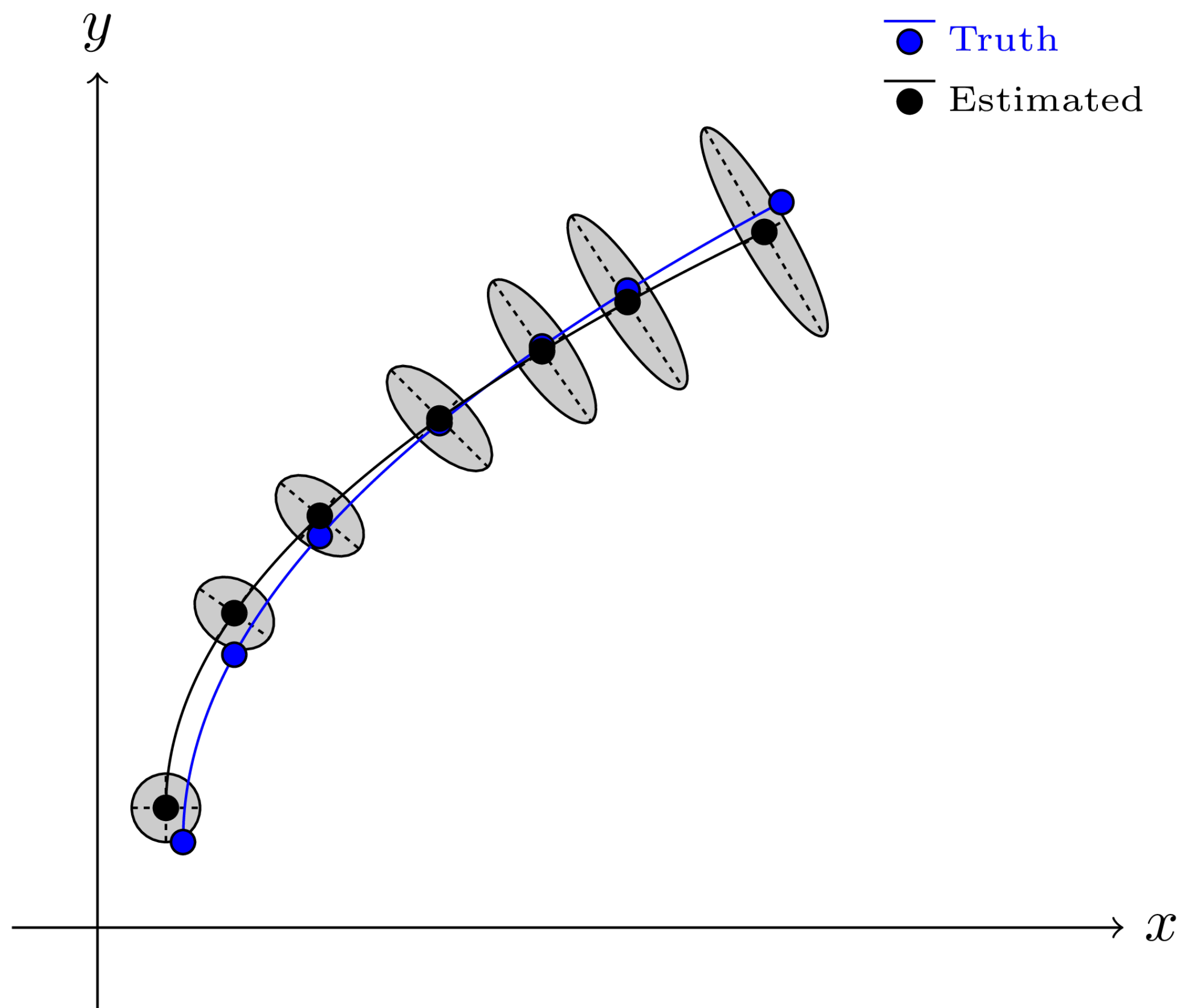
Linearization: $\mathbf{f}(\mathbf{x}, t) \approx \mathbf{f}(\boldsymbol{\mu}, t) + \mathbf{f}'(\boldsymbol{\mu}, t)(\mathbf{x} - \boldsymbol{\mu})$

Observation: $\mathbf{z} = \mathbf{h}(\mathbf{x}, t) + \mathbf{v}(t)$

The Extended Kalman Filter

Assumptions and Limitations

- EKF linearizes the nonlinear system about an estimate mean value, assuming that the observations are frequent enough that the linearization is accurate



Model: $\dot{\mathbf{x}} = \mathbf{f}(\mathbf{x}, t) + \mathbf{w}(t)$

Linearization: $\mathbf{f}(\mathbf{x}, t) \approx \mathbf{f}(\boldsymbol{\mu}, t) + \mathbf{f}'(\boldsymbol{\mu}, t)(\mathbf{x} - \boldsymbol{\mu})$

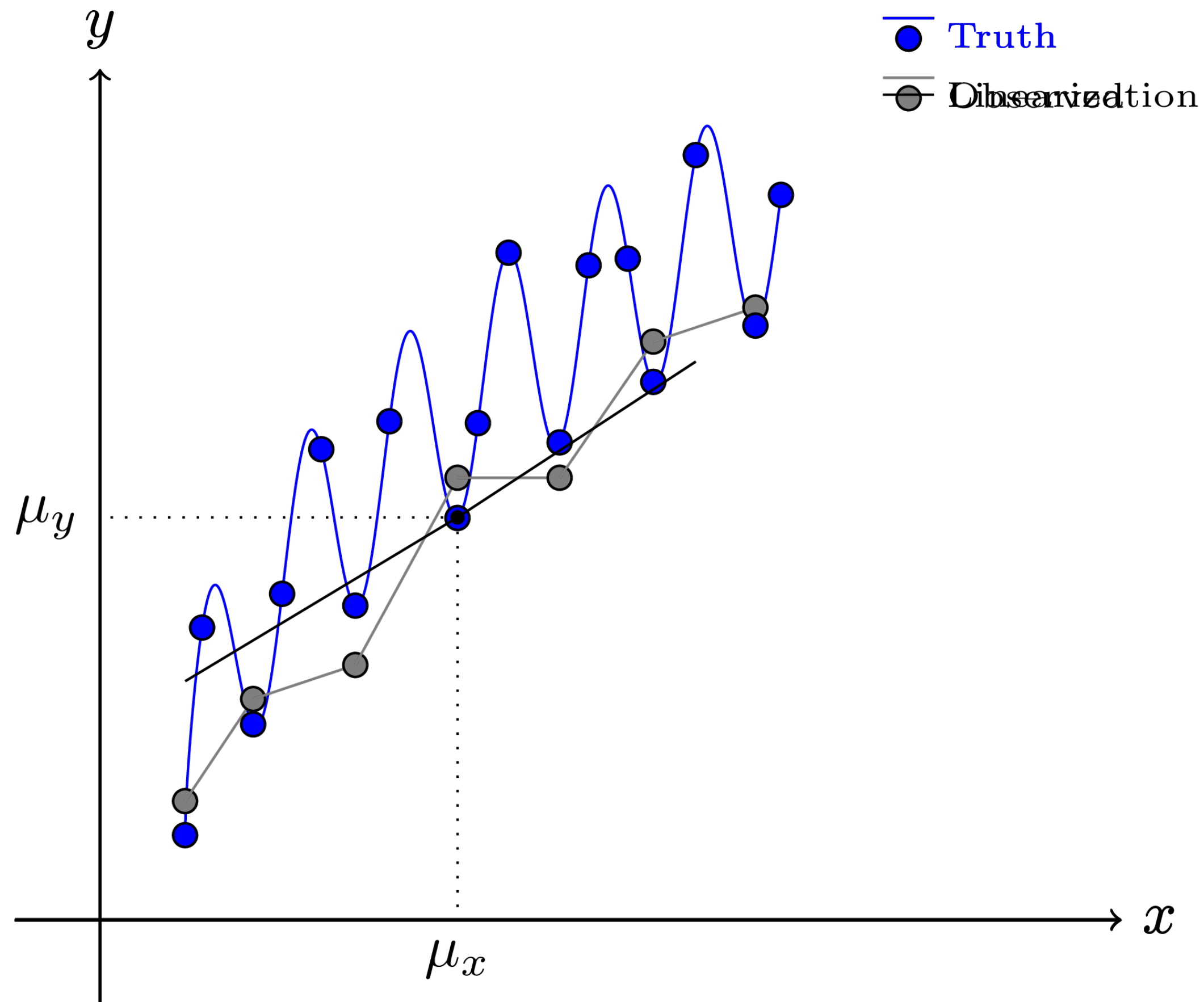
Observation: $\mathbf{z} = \mathbf{h}(\mathbf{x}, t) + \mathbf{v}(t)$

Estimation: $\left\{ \begin{array}{l} \dot{\hat{\mathbf{x}}} = \mathbf{f}(\hat{\mathbf{x}}, t) + \mathbf{K}(t)[\mathbf{z} - \mathbf{h}(\hat{\mathbf{x}})] \\ \dot{\mathbf{P}}(t) = \mathbf{F}(t)\mathbf{P}(t) + \mathbf{P}(t)\mathbf{F}(t)^T - \mathbf{K}(t)\mathbf{H}(t)\mathbf{P}(t) + \mathbf{Q}(t) \\ \mathbf{K}(t) = \mathbf{P}(t)\mathbf{H}(t)^T\mathbf{R}(t)^{-1} \\ \mathbf{F}(t) = \left. \frac{\partial \mathbf{f}}{\partial \mathbf{x}} \right|_{\hat{\mathbf{x}}}, \quad \mathbf{H}(t) = \left. \frac{\partial \mathbf{h}}{\partial \mathbf{x}} \right|_{\hat{\mathbf{x}}} \end{array} \right.$

The Extended Kalman Filter

Assumptions and Limitations

- EKF linearizes the nonlinear system about an estimate mean value, assuming that the observations are frequent enough that the linearization is accurate



Model: $\dot{\mathbf{x}} = \mathbf{f}(\mathbf{x}, t) + \mathbf{w}(t)$

Linearization: $\mathbf{f}(\mathbf{x}, t) \approx \mathbf{f}(\boldsymbol{\mu}, t) + \mathbf{f}'(\boldsymbol{\mu}, t)(\mathbf{x} - \boldsymbol{\mu})$

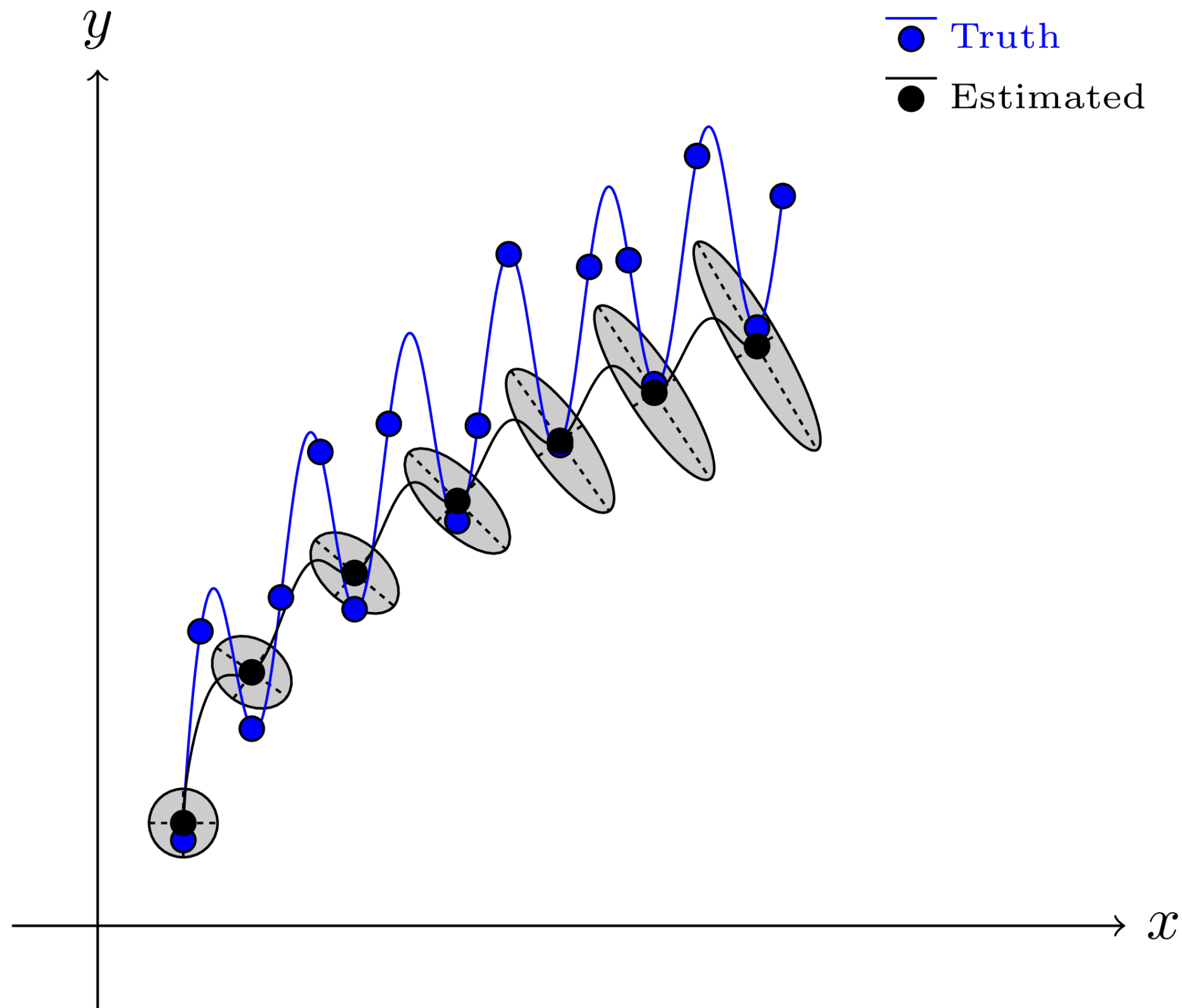
Observation: $\mathbf{z} = \mathbf{h}(\mathbf{x}, t) + \mathbf{v}(t)$

Estimation: $\left\{ \begin{array}{l} \dot{\hat{\mathbf{x}}} = \mathbf{f}(\hat{\mathbf{x}}, t) + \mathbf{K}(t)[\mathbf{z} - \mathbf{h}(\hat{\mathbf{x}})] \\ \dot{\mathbf{P}}(t) = \mathbf{F}(t)\mathbf{P}(t) + \mathbf{P}(t)\mathbf{F}(t)^T - \mathbf{K}(t)\mathbf{H}(t)\mathbf{P}(t) + \mathbf{Q}(t) \\ \mathbf{K}(t) = \mathbf{P}(t)\mathbf{H}(t)^T\mathbf{R}(t)^{-1} \\ \mathbf{F}(t) = \left. \frac{\partial \mathbf{f}}{\partial \mathbf{x}} \right|_{\hat{\mathbf{x}}}, \quad \mathbf{H}(t) = \left. \frac{\partial \mathbf{h}}{\partial \mathbf{x}} \right|_{\hat{\mathbf{x}}} \end{array} \right.$

The Extended Kalman Filter

Assumptions and Limitations

- EKF linearizes the nonlinear system about an estimate mean value, assuming that the observations are frequent enough that the linearization is accurate



Model: $\dot{\mathbf{x}} = \mathbf{f}(\mathbf{x}, t) + \mathbf{w}(t)$

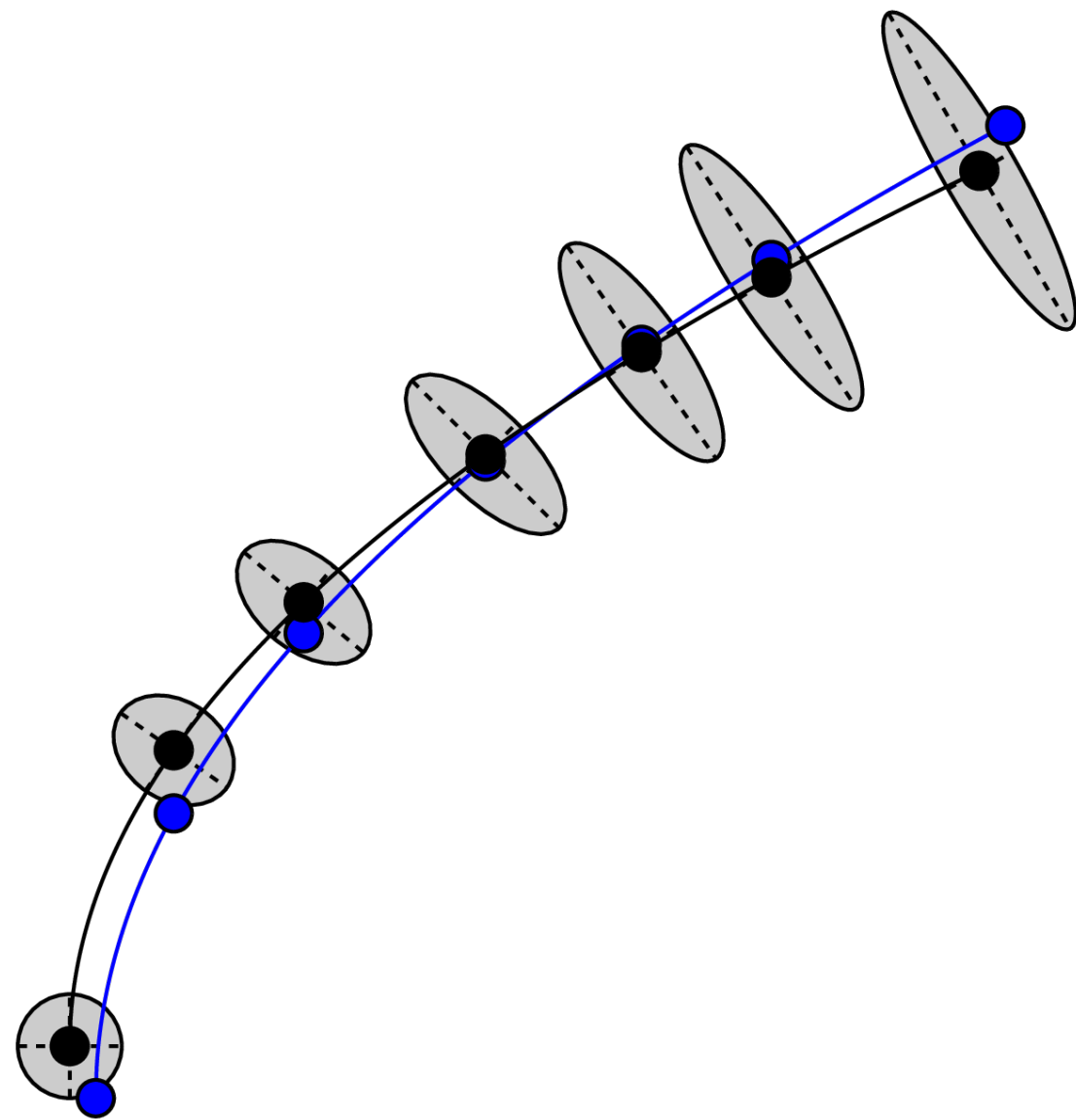
Linearization: $\mathbf{f}(\mathbf{x}, t) \approx \mathbf{f}(\boldsymbol{\mu}, t) + \mathbf{f}'(\boldsymbol{\mu}, t)(\mathbf{x} - \boldsymbol{\mu})$

Observation: $\mathbf{z} = \mathbf{h}(\mathbf{x}, t) + \mathbf{v}(t)$

Estimation: $\left\{ \begin{array}{l} \dot{\hat{\mathbf{x}}} = \mathbf{f}(\hat{\mathbf{x}}, t) + \mathbf{K}(t)[\mathbf{z} - \mathbf{h}(\hat{\mathbf{x}})] \\ \dot{\mathbf{P}}(t) = \mathbf{F}(t)\mathbf{P}(t) + \mathbf{P}(t)\mathbf{F}(t)^T - \mathbf{K}(t)\mathbf{H}(t)\mathbf{P}(t) + \mathbf{Q}(t) \\ \mathbf{K}(t) = \mathbf{P}(t)\mathbf{H}(t)^T\mathbf{R}(t)^{-1} \\ \mathbf{F}(t) = \left. \frac{\partial \mathbf{f}}{\partial \mathbf{x}} \right|_{\hat{\mathbf{x}}}, \quad \mathbf{H}(t) = \left. \frac{\partial \mathbf{h}}{\partial \mathbf{x}} \right|_{\hat{\mathbf{x}}} \end{array} \right.$

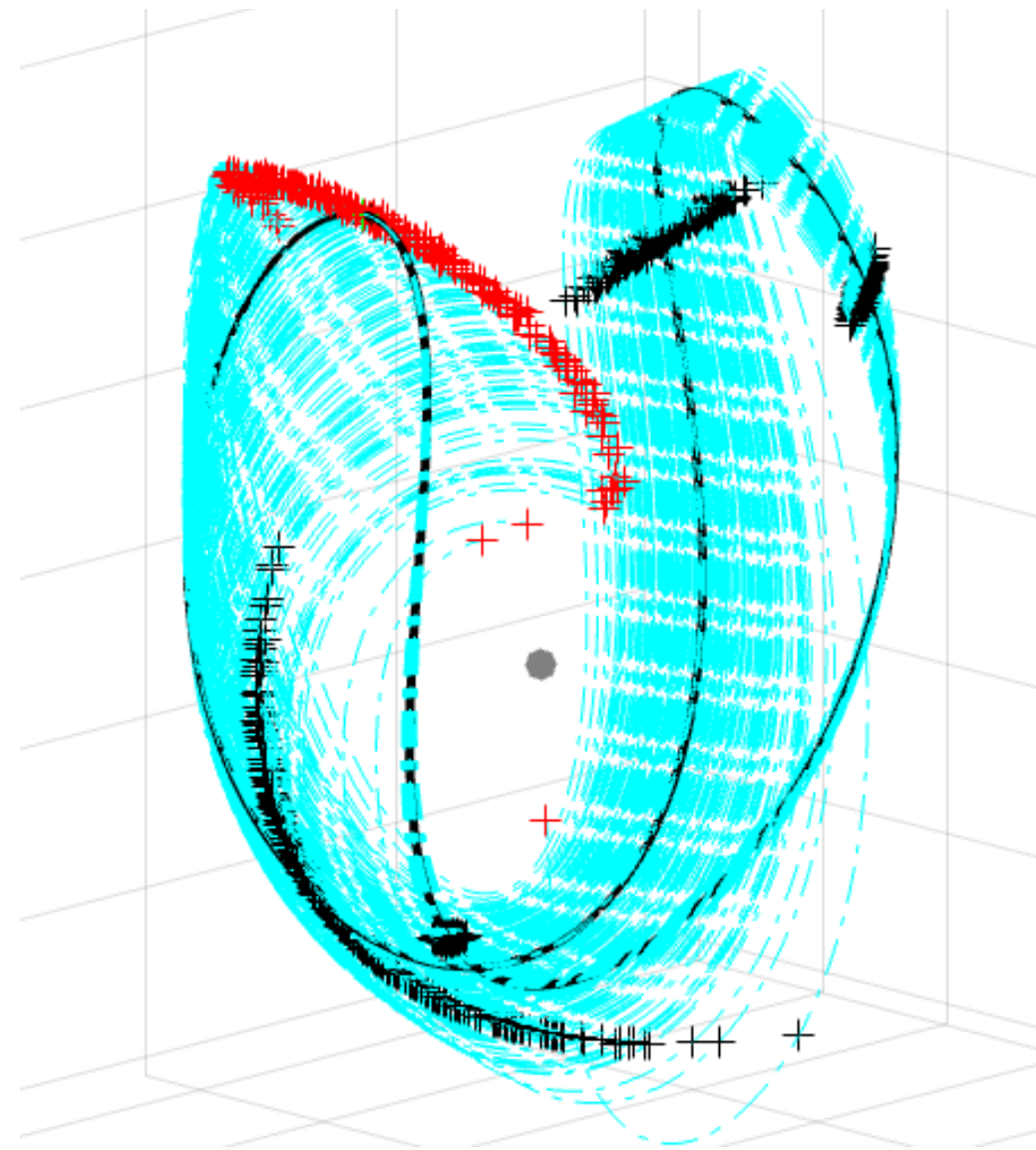
- For the majority of past space missions, the observation frequency has made linearization error negligible - **this may not always be the case!**

Kalman Filters Variations



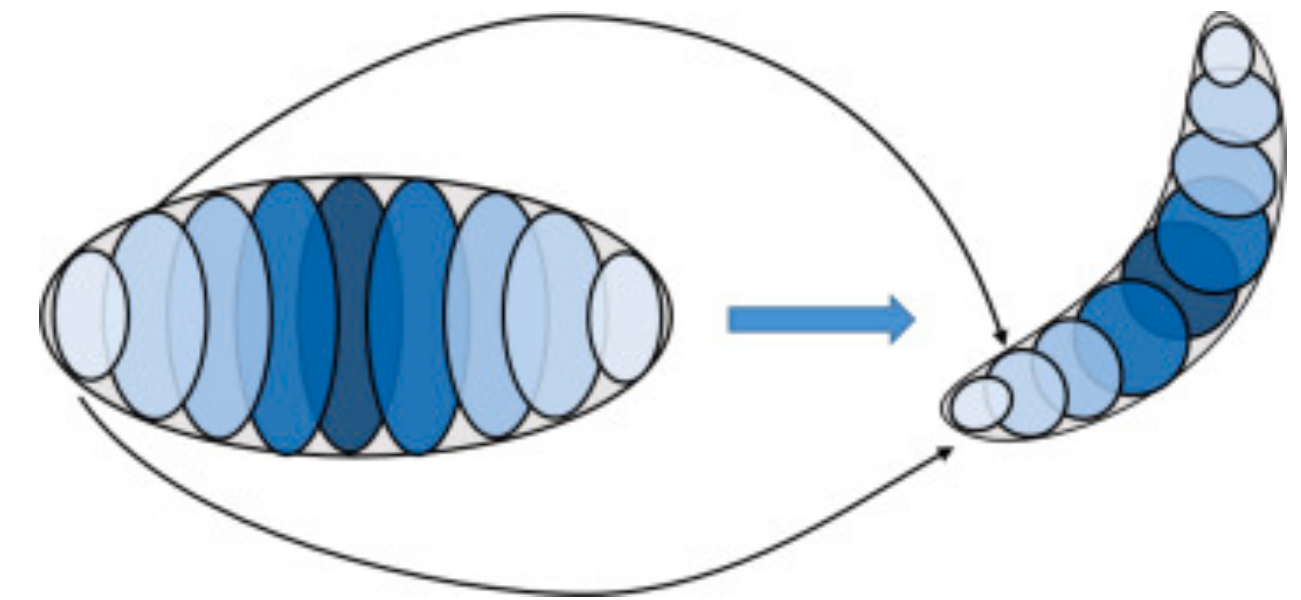
- Accuracy is predicated on frequent measurement updates such that linearization errors are negligible
- Extremely chaotic dynamics means the **measurement frequency requirement** may not be feasible for certain regimes

Monte Carlo/Particle Filters



- “Monte Carlo has some core fundamental limitations... the computational burden becomes prohibitive for very low probability events.” - NASA Technology Roadmaps, 2015
- A large, **static** number of particles are required to represent non-Gaussian uncertainty

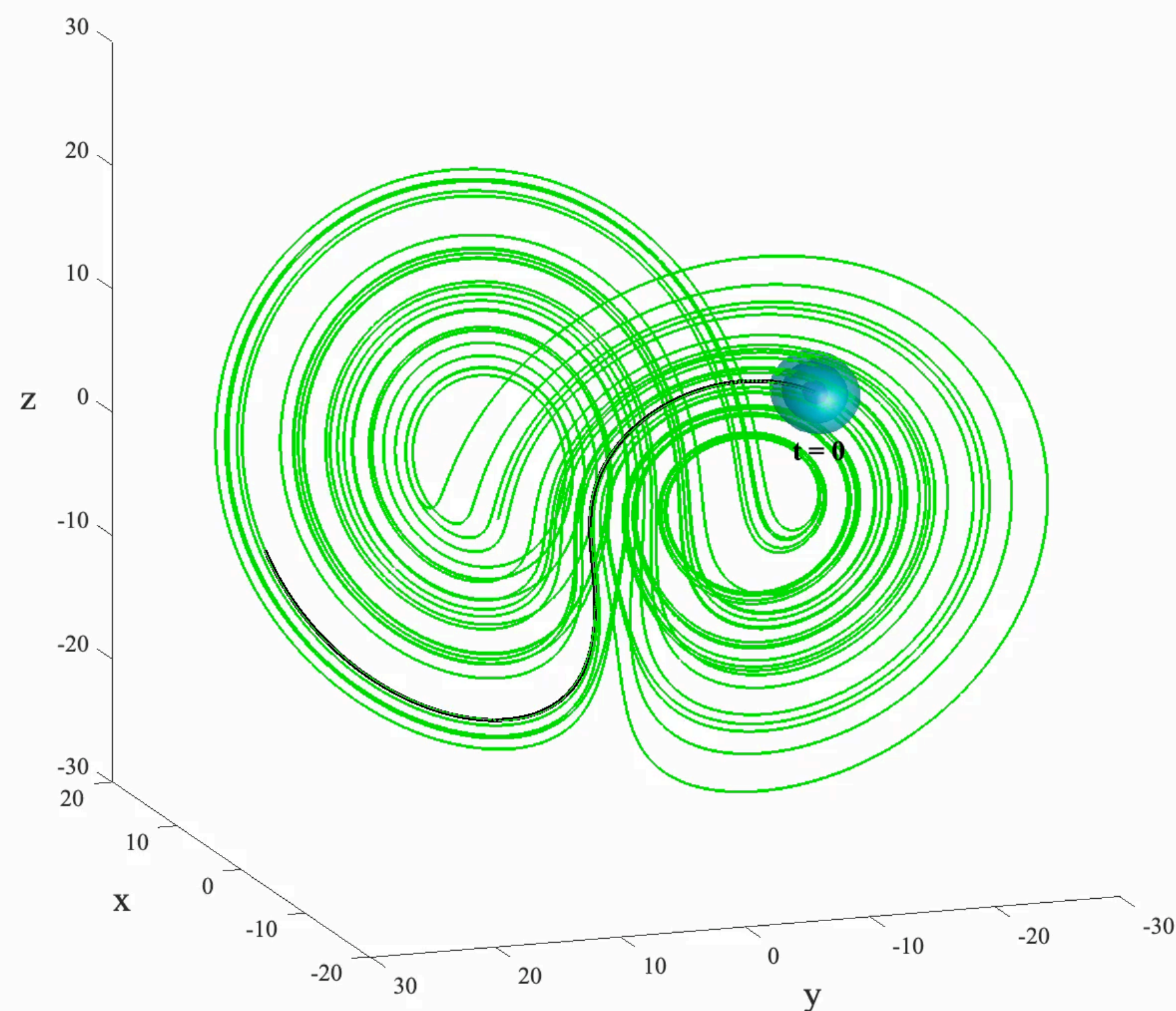
Gaussian Mixture Models



- Depicts a non-Gaussian uncertainty as a mixture of Gaussian distributions
- Representing highly non-Gaussian distributions requires a large number of Gaussian distributions, equating to an **ad-hoc splitting/weighting procedure** and a computational burden

Efficient, Non-Gaussian, Uncertainty Propagation Methods

- To represent state uncertainty in chaotic regimes, novel uncertainty propagation methods must be accurate for long periods of time in the **absence of measurement updates**, represent **non-Gaussian distributions**, consider **epistemic uncertainty**, and be **scalable to high-dimensional problems**.



Grid-based Bayesian Estimation Exploiting Sparsity (GBEES)

An efficient Bayesian estimation method for representing and propagating uncertainty



General Formulation

Mixed Discrete/Continuous Propagation

- GBEEES consists of two distinct processes, one performed in **continuous-time**, the other in **discrete-time**:

1. The probability distribution function $p_{\mathbf{x}}(\mathbf{x}', t)$ is continuous-time marched via the **Fokker-Planck Equation**:

$$\frac{\partial p_{\mathbf{x}}(\mathbf{x}', t)}{\partial t} = - \frac{\partial f_i(\mathbf{x}', t) p_{\mathbf{x}}(\mathbf{x}', t)}{\partial x'_i} + \frac{1}{2} \frac{\partial^2 q_{ij} p_{\mathbf{x}}(\mathbf{x}', t)}{\partial x'_i \partial x'_j}$$

- f_i : advection (EOMs) in the i^{th} dimension
- q_{ij} : $(i, j)^{\text{th}}$ element of the spectral density ($Q = 0$, PDE is hyperbolic)

2. At discrete-time interval t_k , measurement y_k updates $p_{\mathbf{x}}(\mathbf{x}', t)$ via **Bayes' Theorem**:

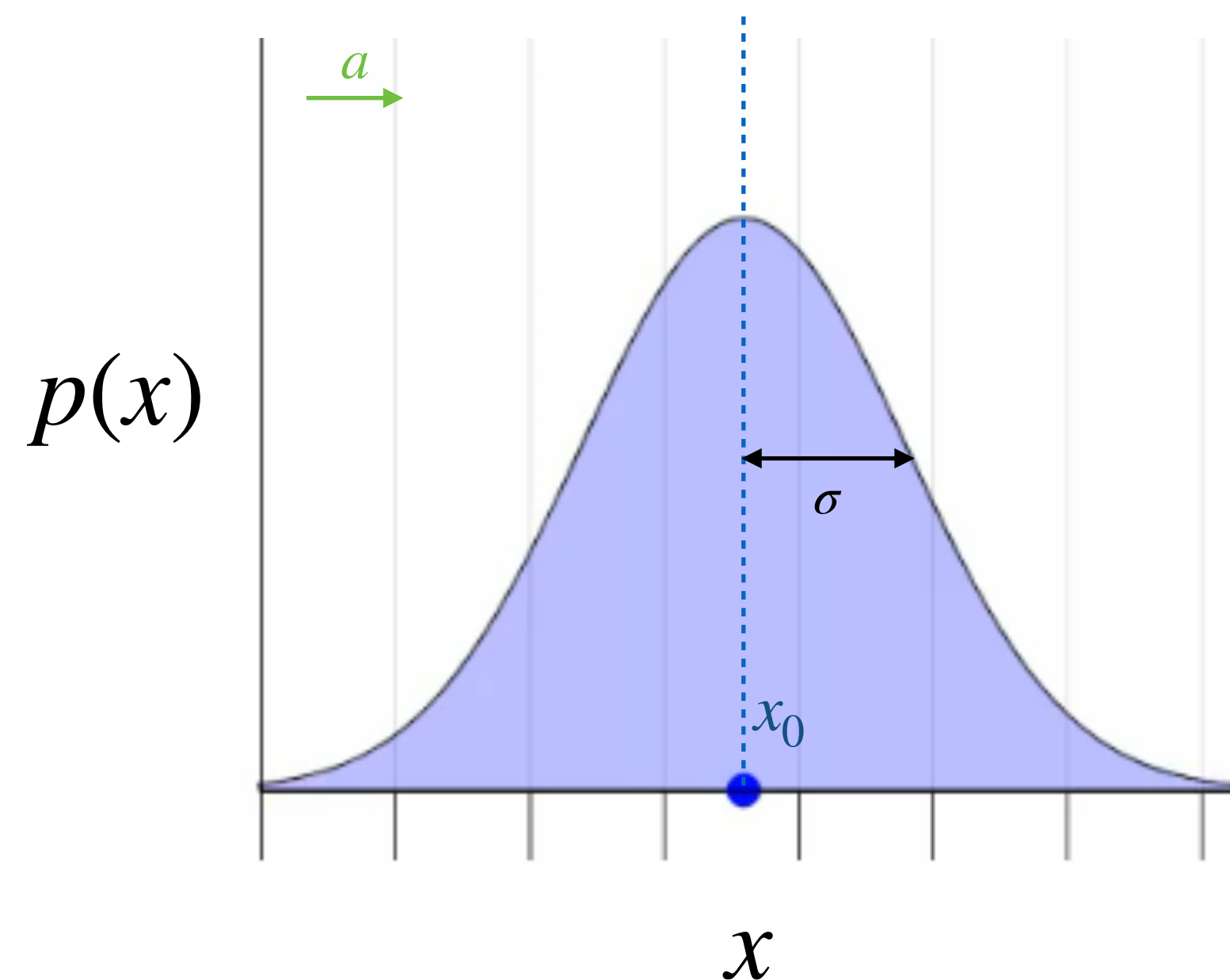
$$p_{\mathbf{x}}(\mathbf{x}', t_{k+}) = \frac{p_{\mathbf{y}}(\mathbf{y}_k | \mathbf{x}') p_{\mathbf{x}}(\mathbf{x}', t_{k-})}{C}$$

- $p_{\mathbf{x}}(\mathbf{x}', t_{k+})$: a posteriori distribution
- $p_{\mathbf{y}}(\mathbf{y}_k | \mathbf{x}')$: measurement distribution
- $p_{\mathbf{x}}(\mathbf{x}', t_{k-})$: a priori distribution
- C : normalization constant

- Consider a 1-dimensional, linear test example:

$$\mathbf{x} = [x], \quad \frac{d\mathbf{x}}{dt} = [a], \quad a > 0$$

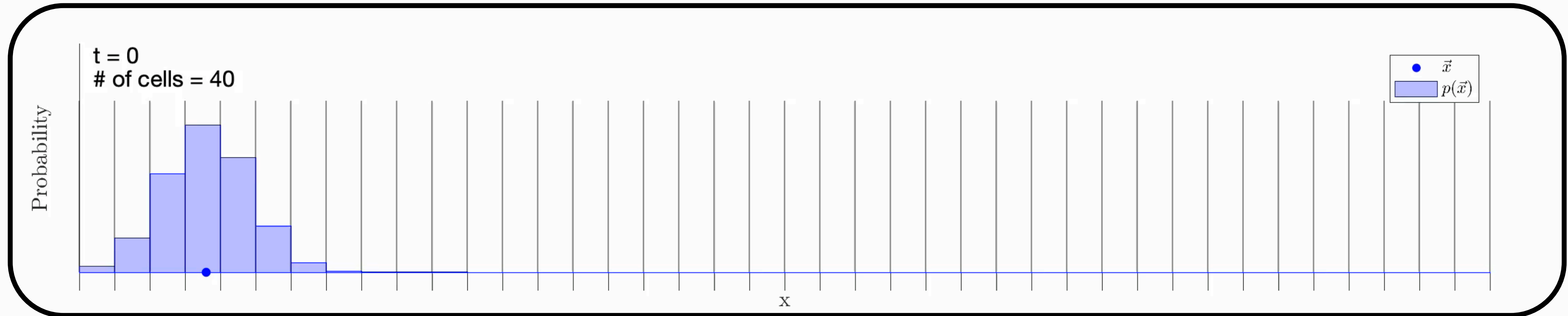
- Initial observation of $x(t)$ results in a Gaussian PDF $p(x)$ centered about x_0 with standard deviation σ



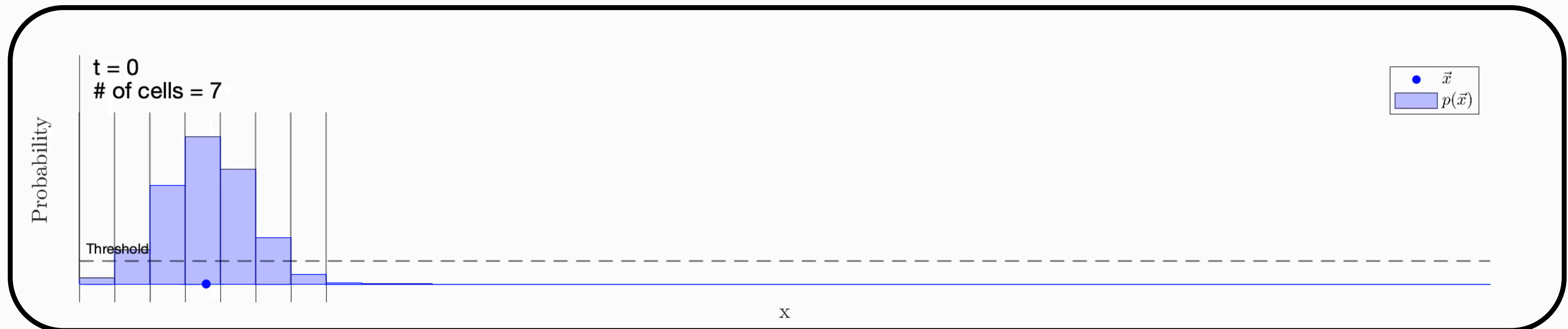
- How does $p(x)$, governed by $d\mathbf{x}/dt$, change with respect to t ?

GBEES treats probability as a fluid, and time-evolves the distribution subject to the Fokker-Planck Equation via a Godunov, 2nd order-accurate, finite volume method.

- Ignoring sparsity



- Exploiting sparsity

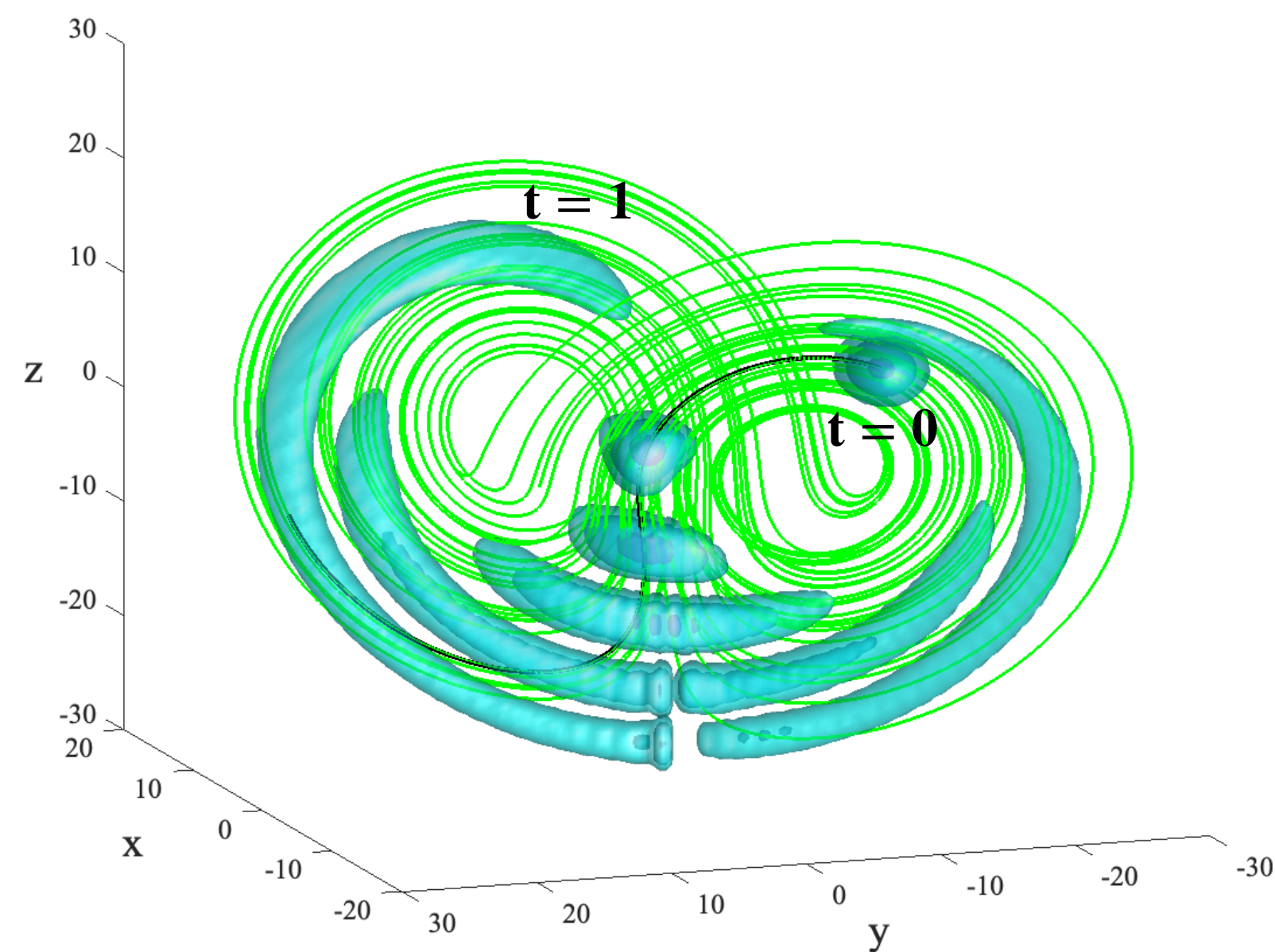


Test Case

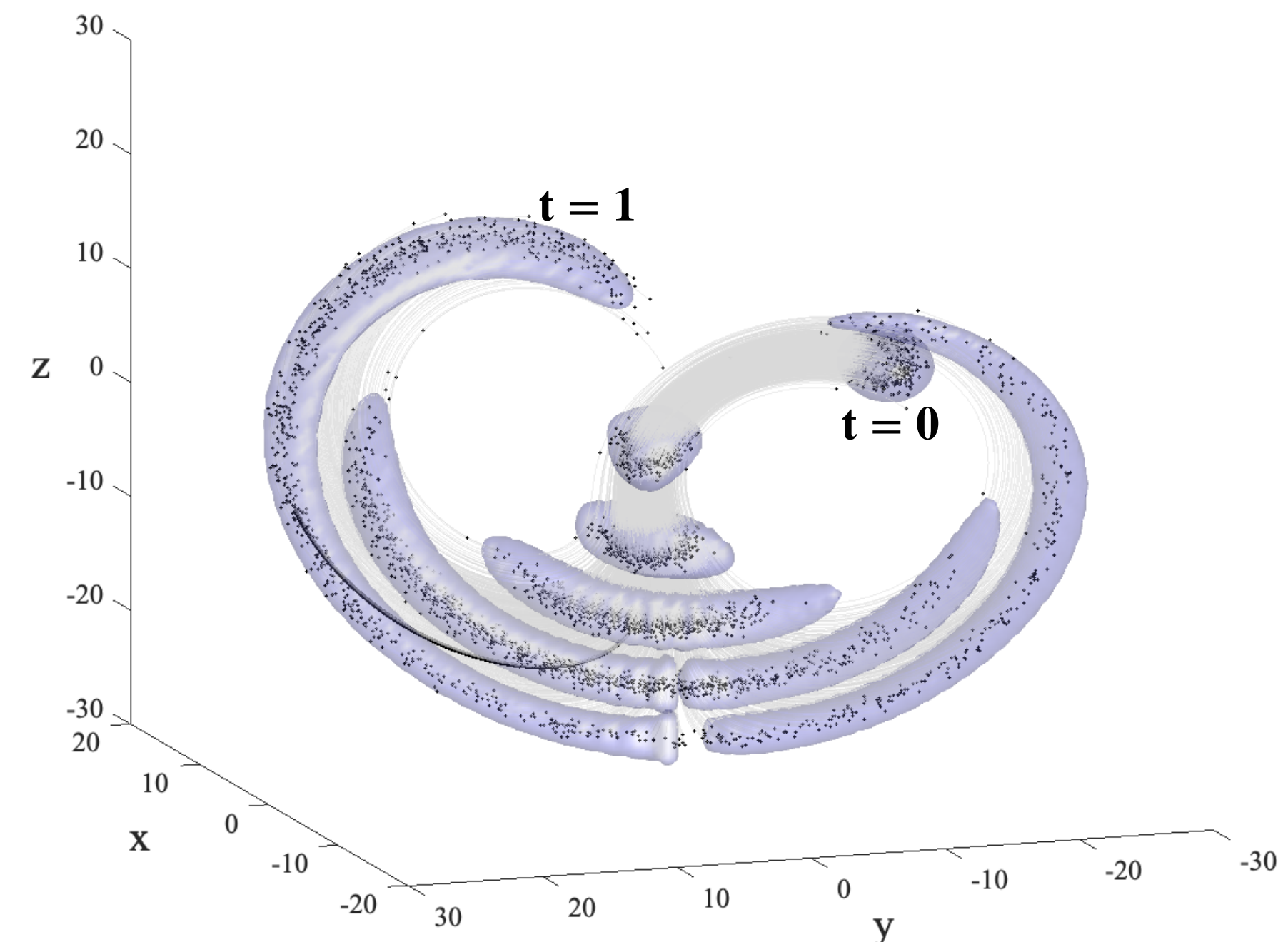
3D Lorenz Attractor

- Colloquially known as the “Butterfly Effect”, the Lorenz attractor is a set of **chaotic** solutions to the Lorenz system
- Test case demonstrates how a Gaussian uncertainty can quickly evolve into a **non-Gaussian uncertainty** (and even split)

$$\mathbf{x} = \begin{bmatrix} x \\ y \\ z \end{bmatrix}, \quad \frac{d\mathbf{x}}{dt} = \begin{bmatrix} \sigma(y - x) \\ -y - xz \\ -b(z + r) - xy \end{bmatrix}$$



$\sigma = 4, b = 1, r = 48$



GBEES compared with a 500 particle Monte Carlo simulation

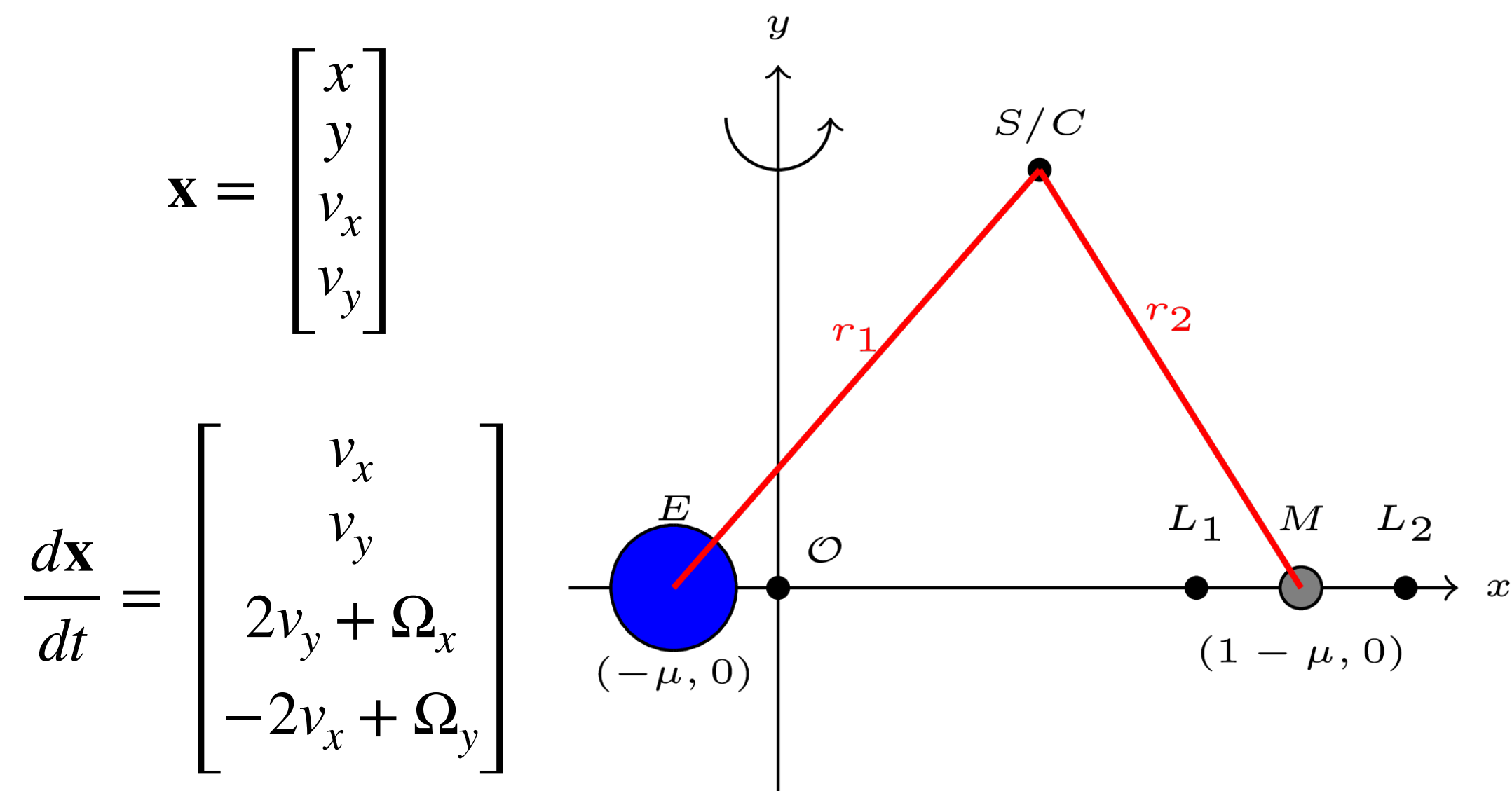
Extension to Astrodynamical Problems

Planar Circular Restricted Three-body Problem (PCR3BP)

- Jump from low-dimensional, theoretical nonlinear systems to high-dimensional, physical nonlinear systems
- As an astrodynamical test case, we apply GBEES to the planar circular restricted three-body problem (PCR3BP)

PCR3BP

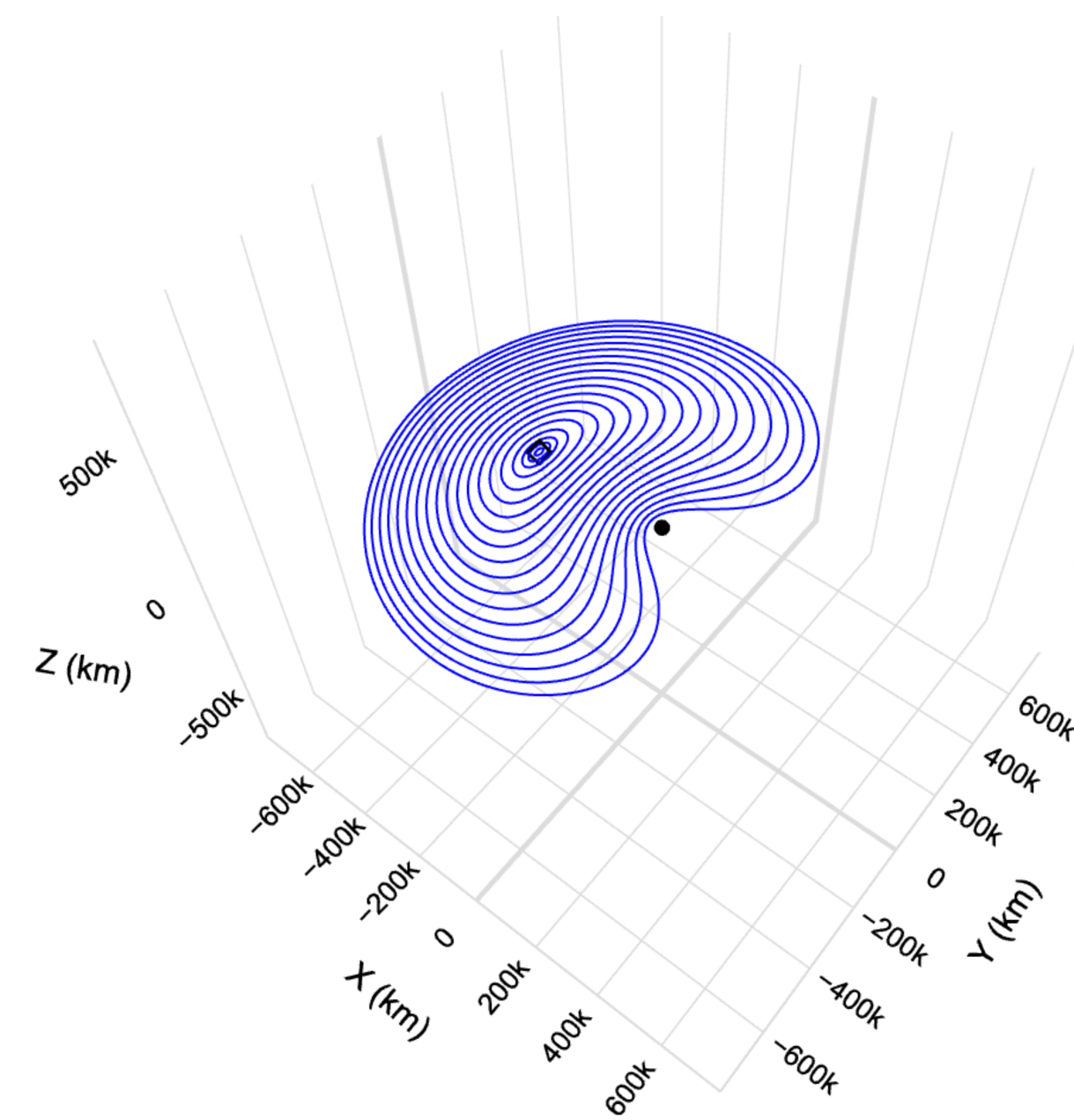
Four-dimensional, nonlinear system



where
$$\Omega(x, y) = \frac{x^2 + y^2}{2} + \frac{1 - \mu}{r_1} + \frac{\mu}{r_2} + \frac{\mu(1 - \mu)}{2}$$

Lyapunov Orbits

Dynamically unstable, entirely planar orbits about the Lagrange points

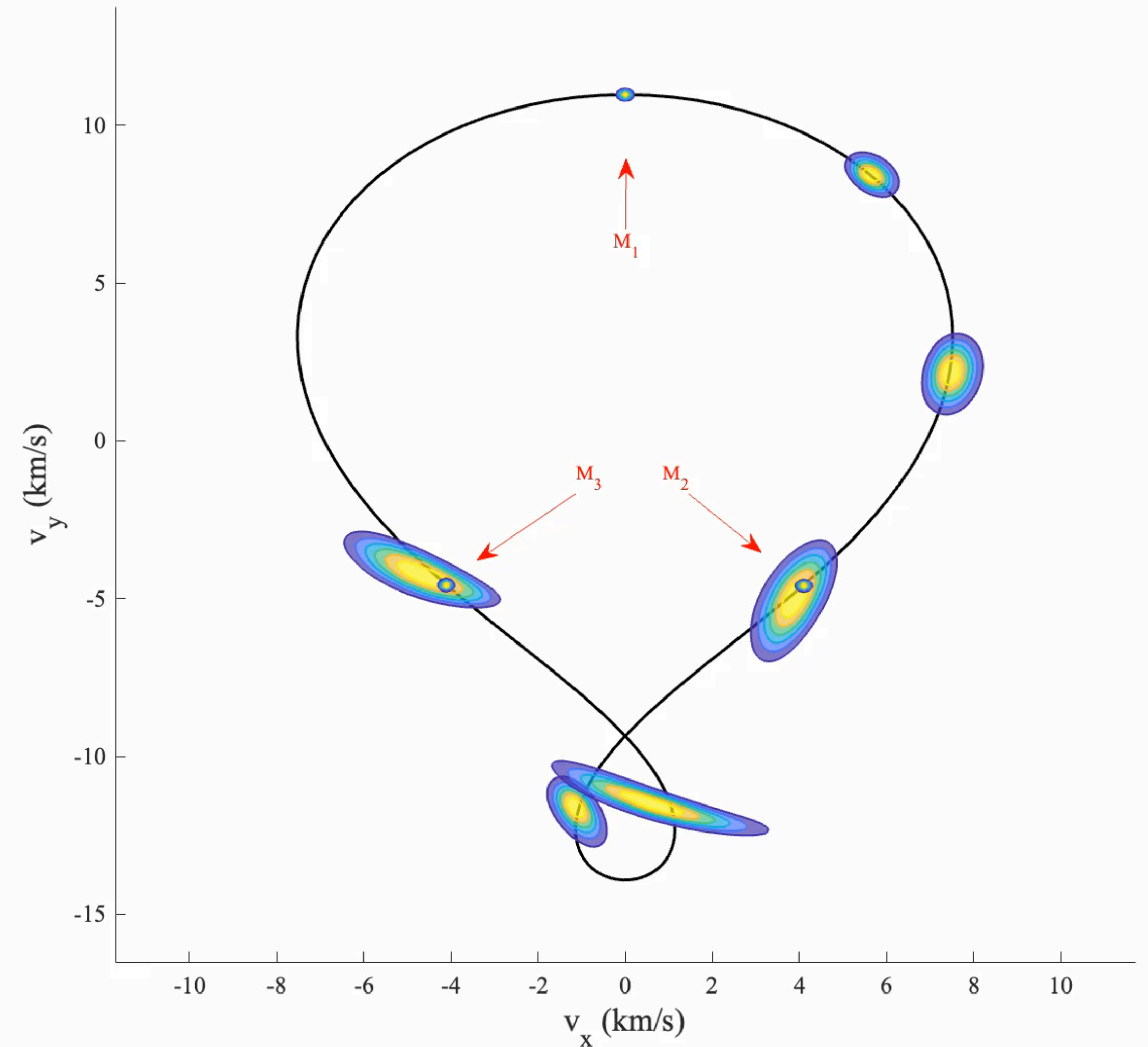
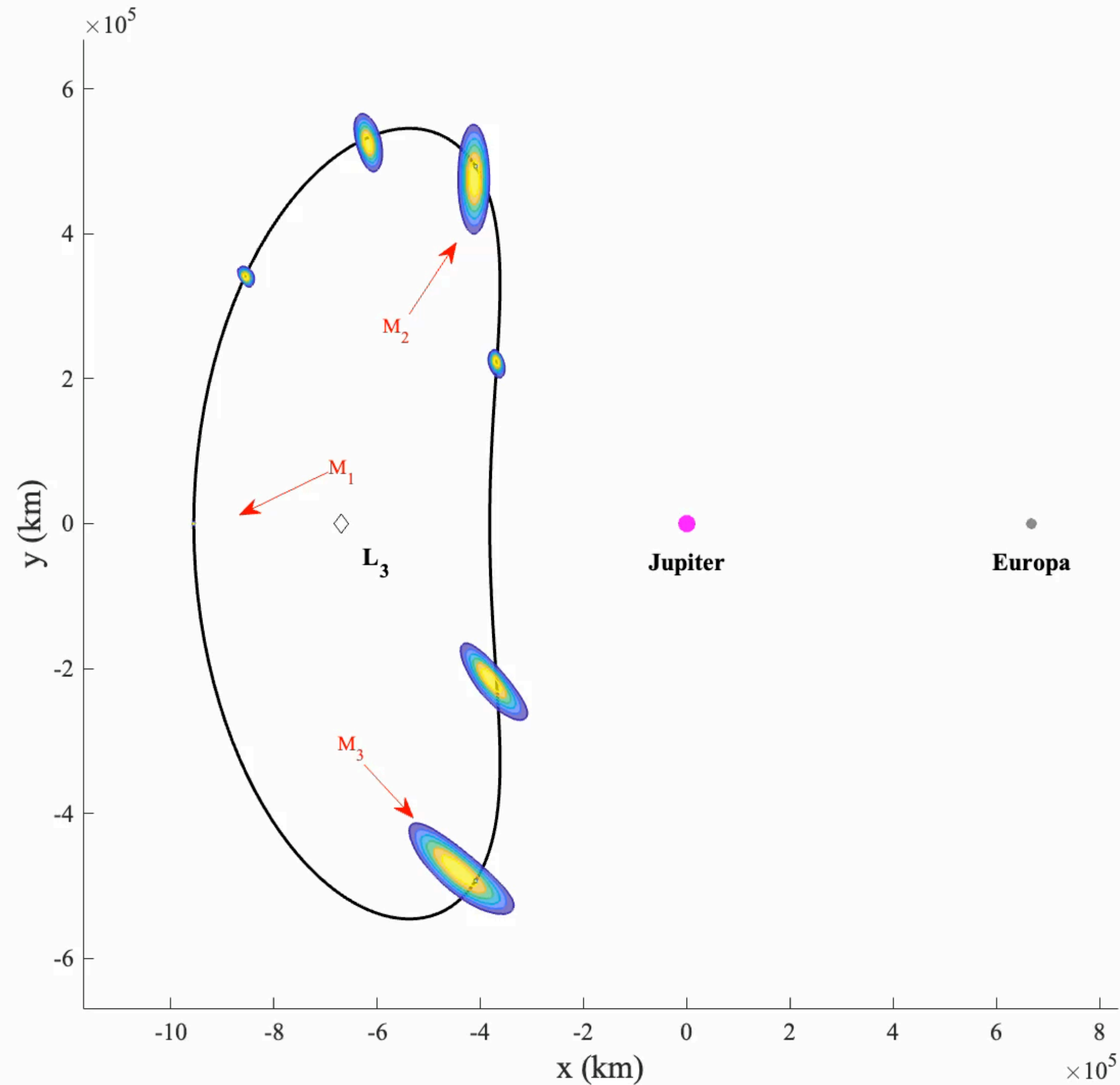


Possible operating trajectories for spacecraft examining celestial systems for multiple orbits - a **great test case for GBEES!**

*Initial conditions generated via JPL Three-Body Periodic Orbit Catalog

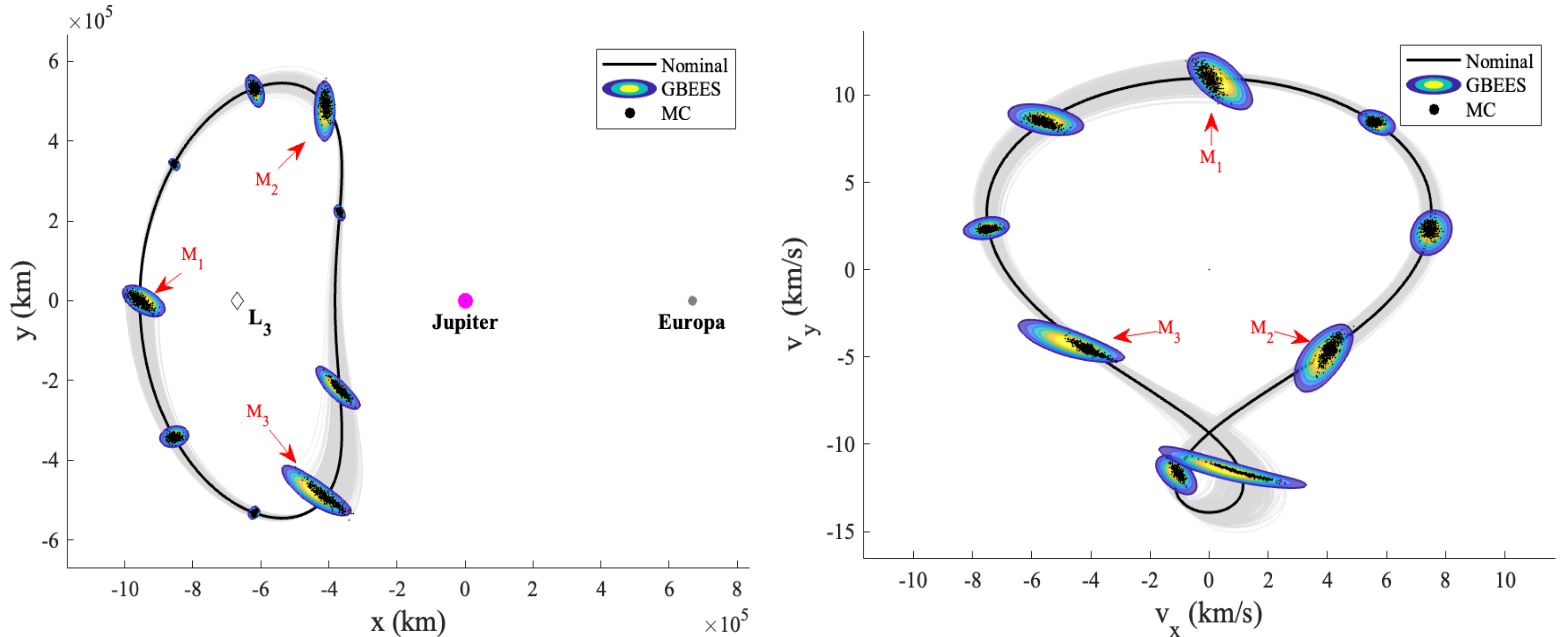
Application of GBEES

Measurement 3, $t=56.5032$ hr



Comparison with MC Simulation - Accuracy

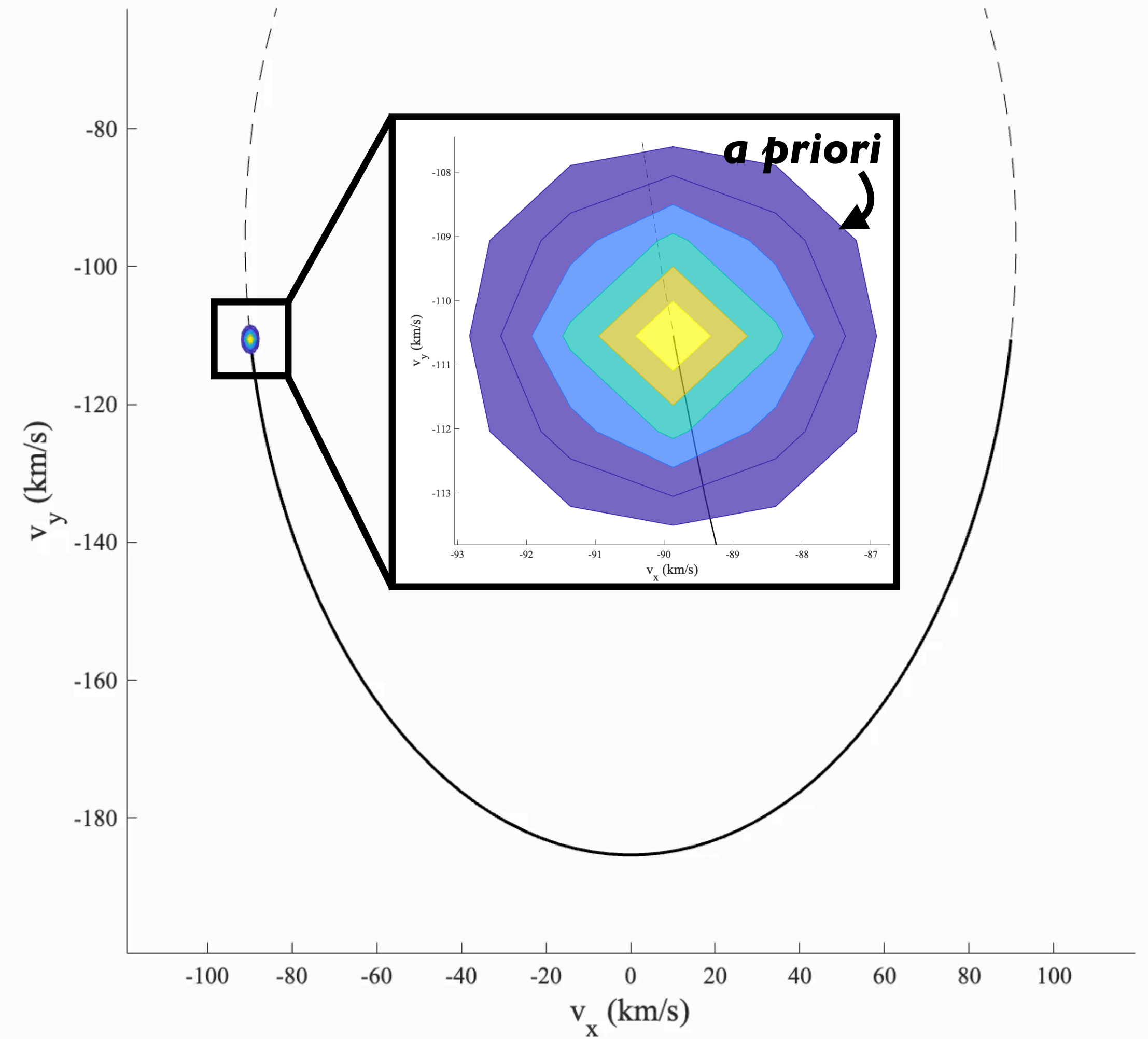
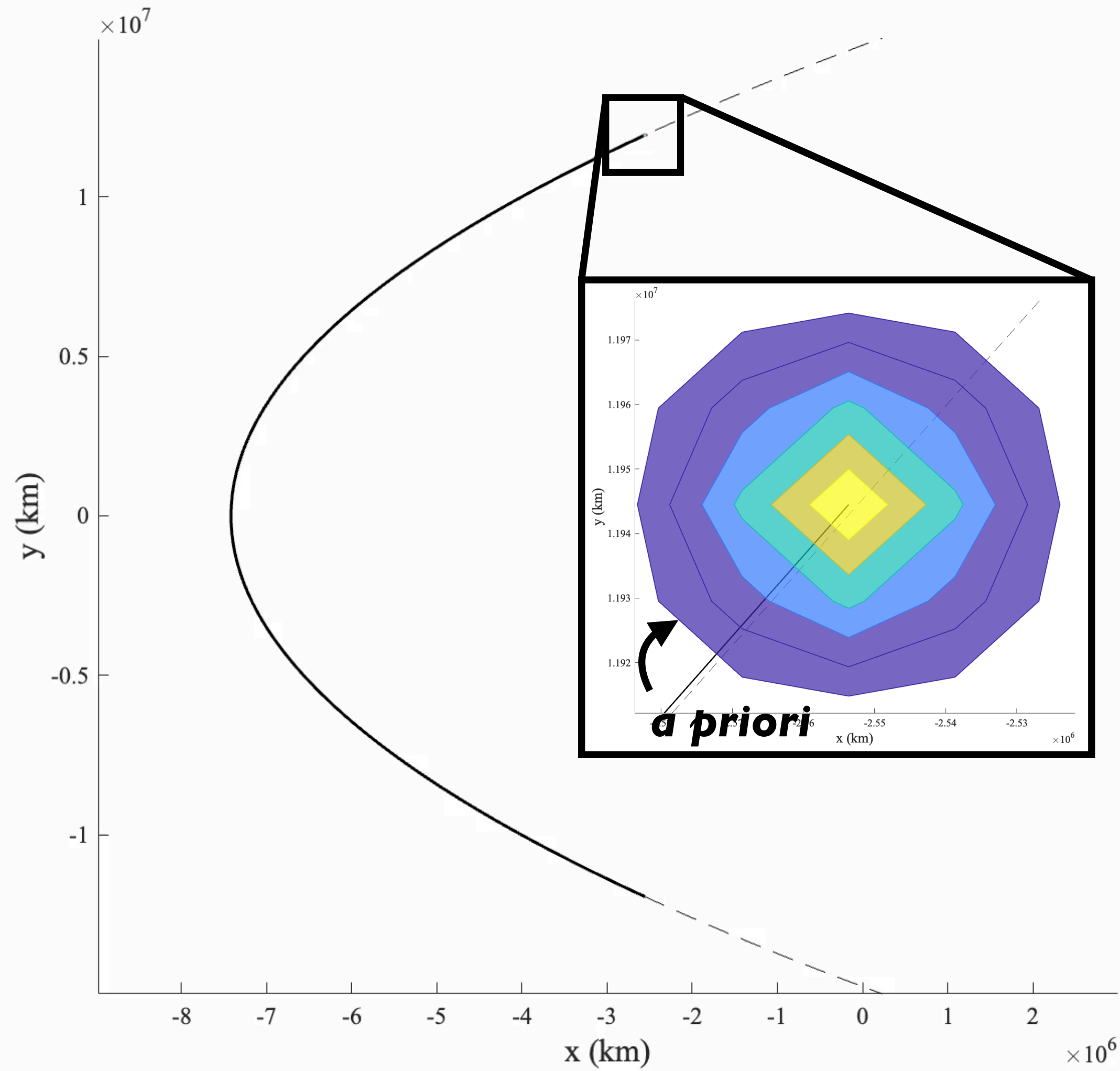
- Comparing results of discretized PDFs propagated via GBEES with 500 particle MC simulation



- Note:** at discrete measurement intervals M_i , GBEES updates the PDF via Bayes' theorem, while the MC simulation resamples from the new *a priori* measurement, disregarding any prior information

Application of GBEEs

Measurement 1, $t=0.0000$ hr





Consideration of epistemic uncertainty for solar probes

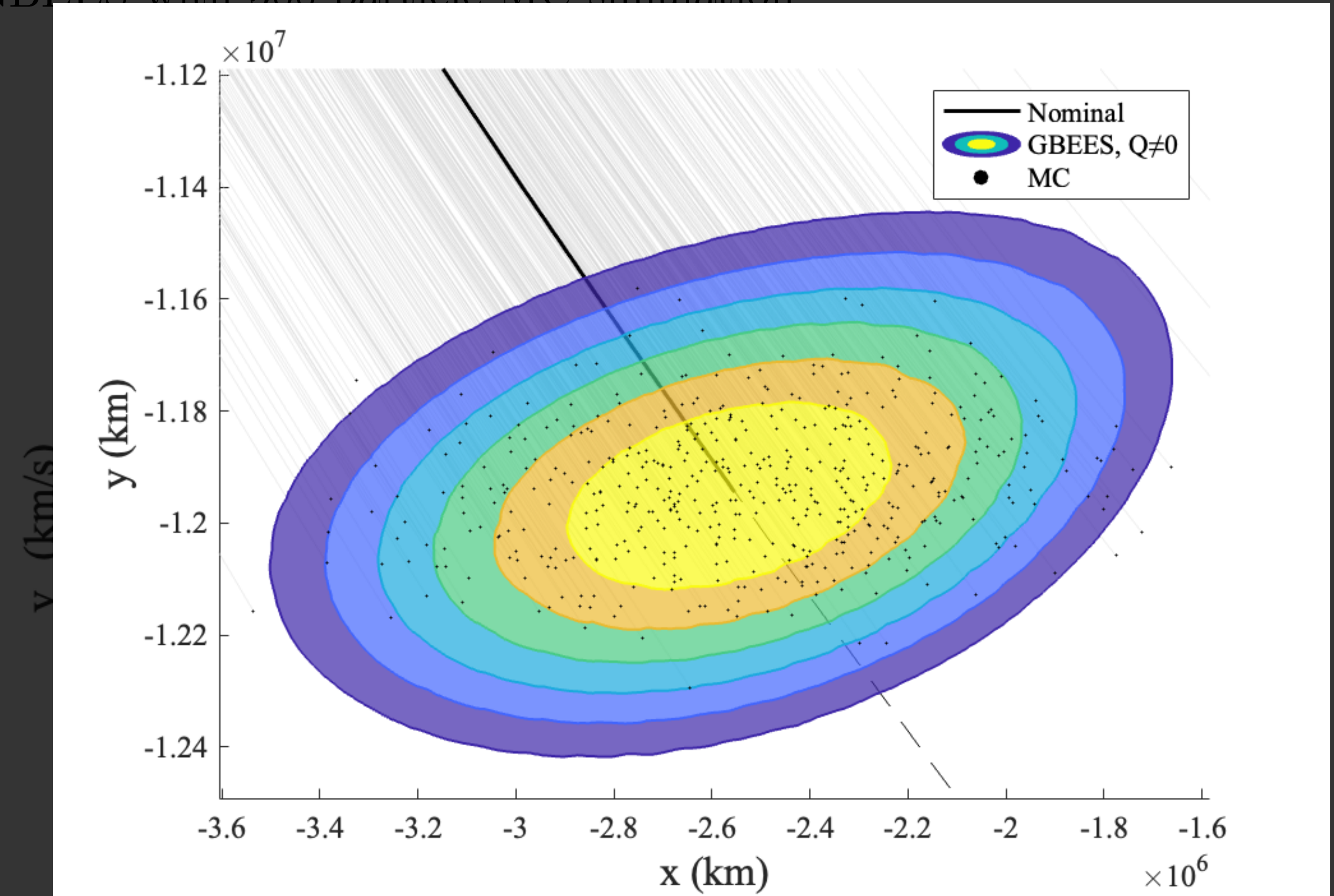
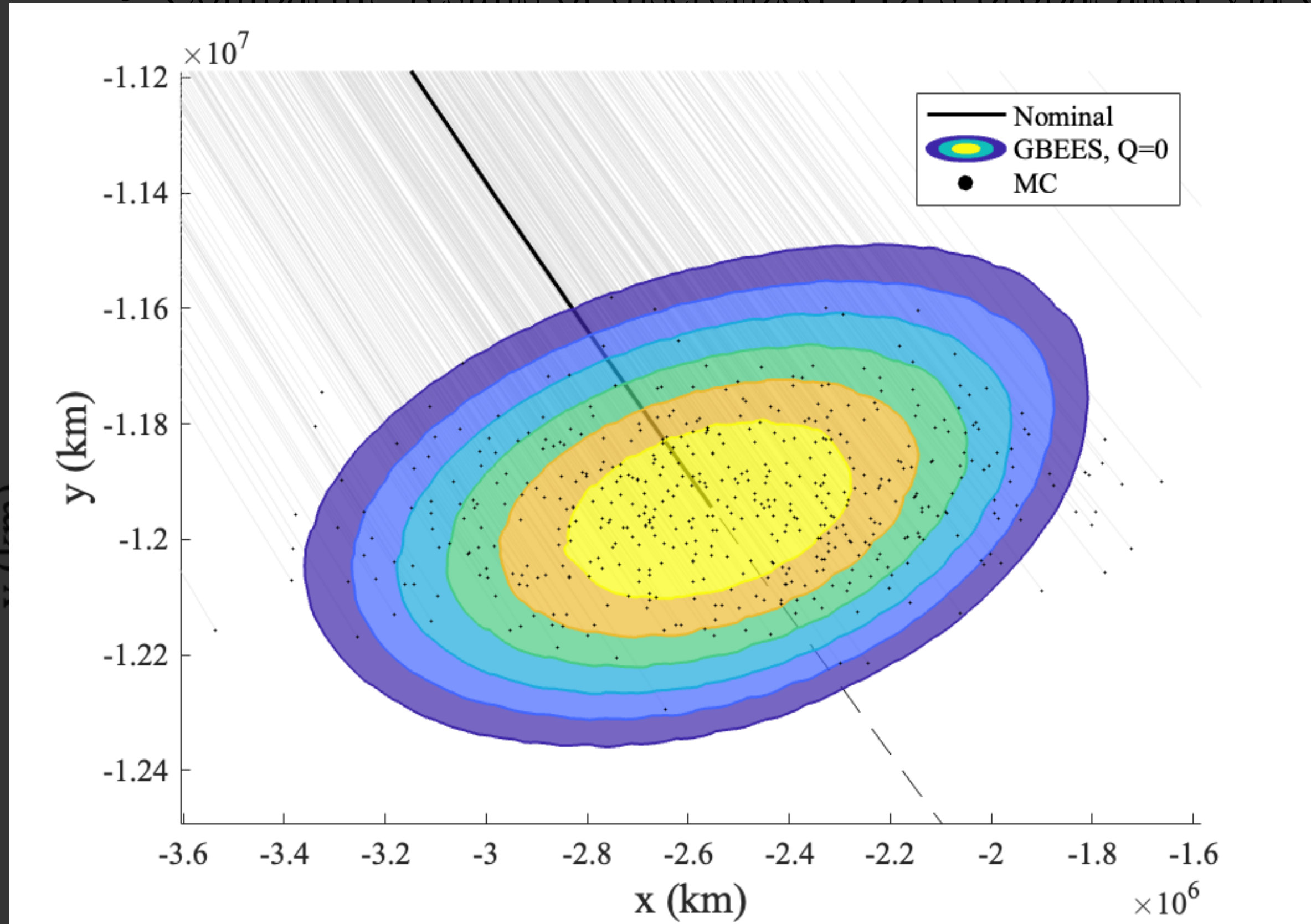


Comparison with MC Simulation - Accuracy

No Diffusion

Diffusion

- Comparing results of discretized PDFs propagated via GBEES with 500 particle MC simulation



- x -position range: $[-3.4136 \times 10^6, -1.7636 \times 10^6]$
- y -position range: $[-1.2416 \times 10^7, -1.1416 \times 10^7]$

- x -position range: $[-3.5836 \times 10^6, -1.5536 \times 10^6]$
- y -position range: $[-1.2536 \times 10^7, -1.1406 \times 10^7]$

• **Note:** there is no consideration for epistemic uncertainty in the MC simulation

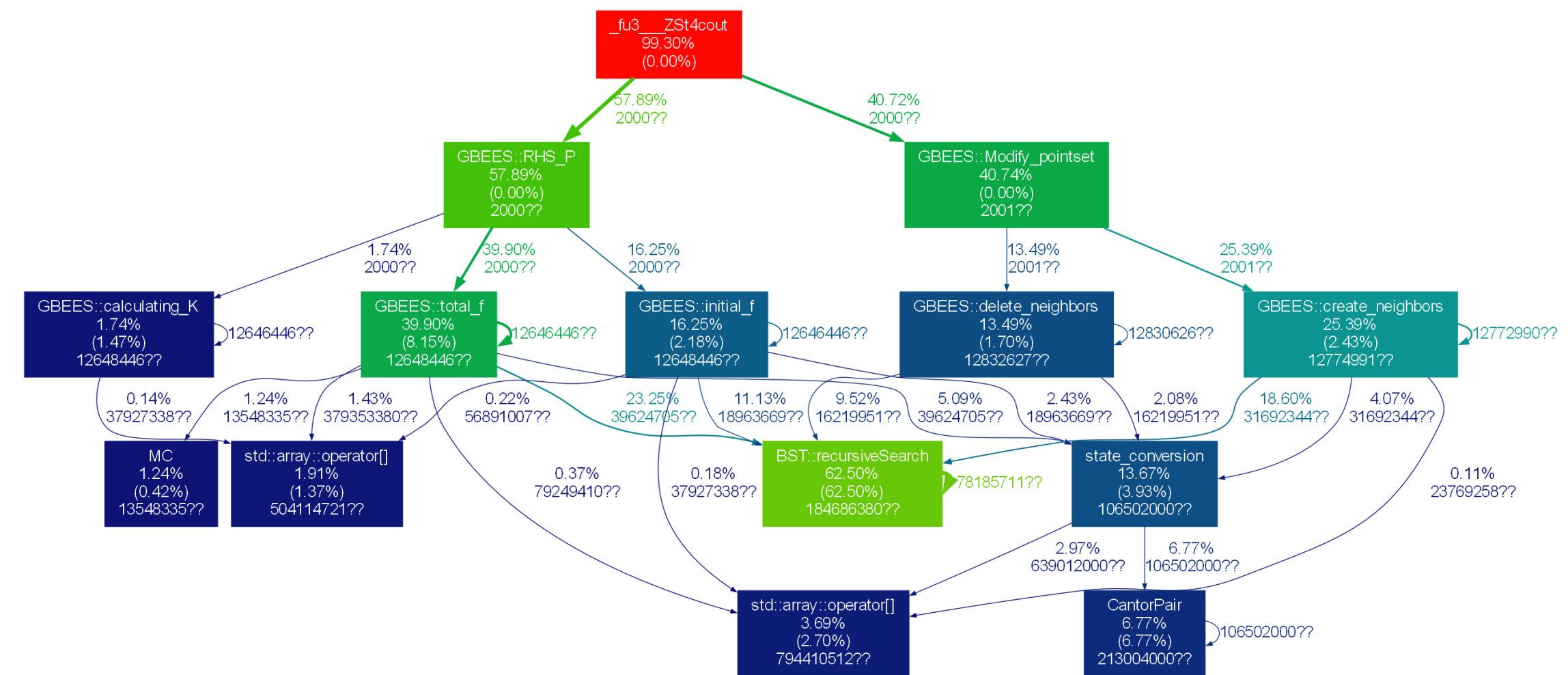
Difference of 380,000 km and 13,000 km in x - and y -directions, respectively!

Conclusion

Comments on Results and Future Work

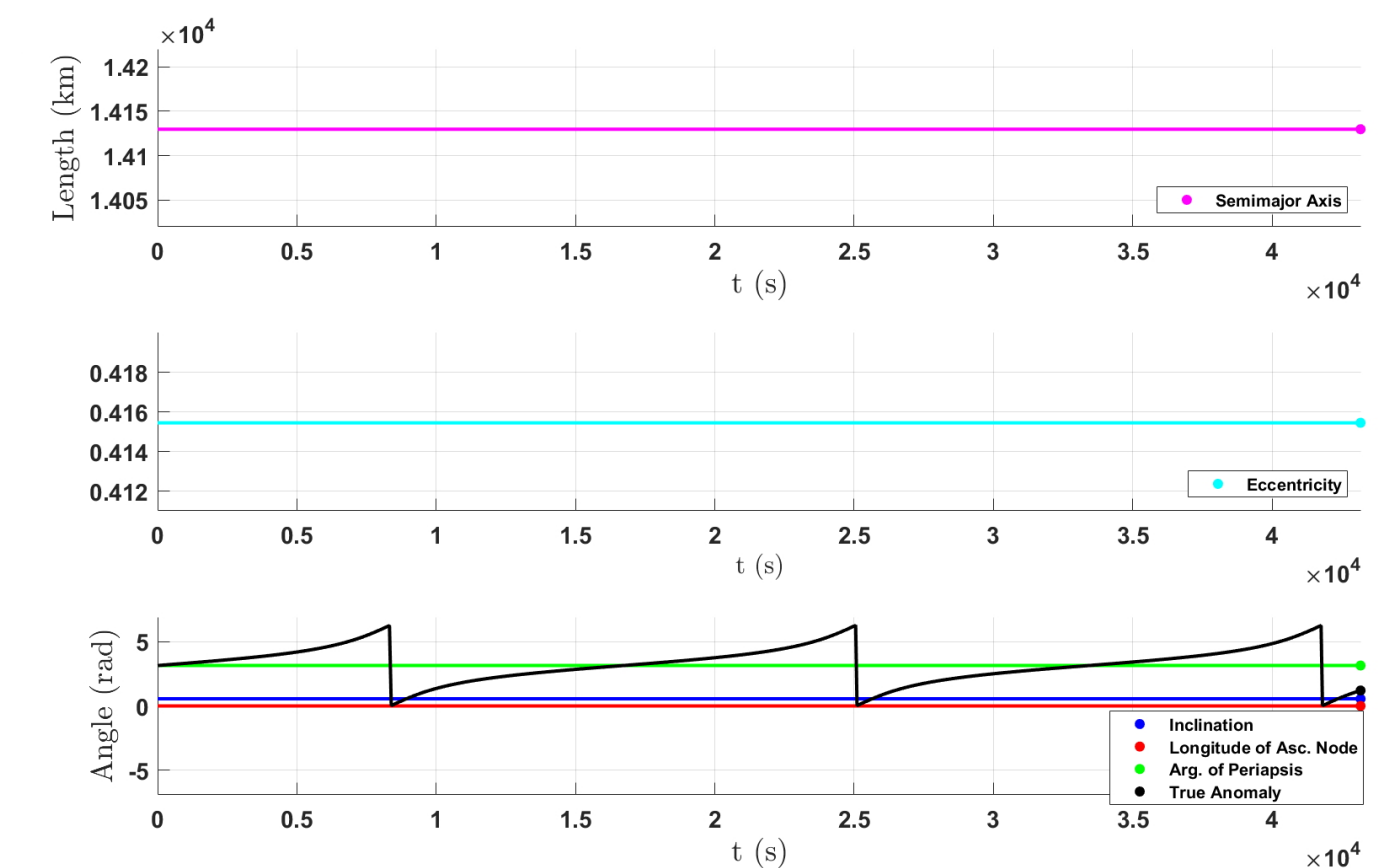
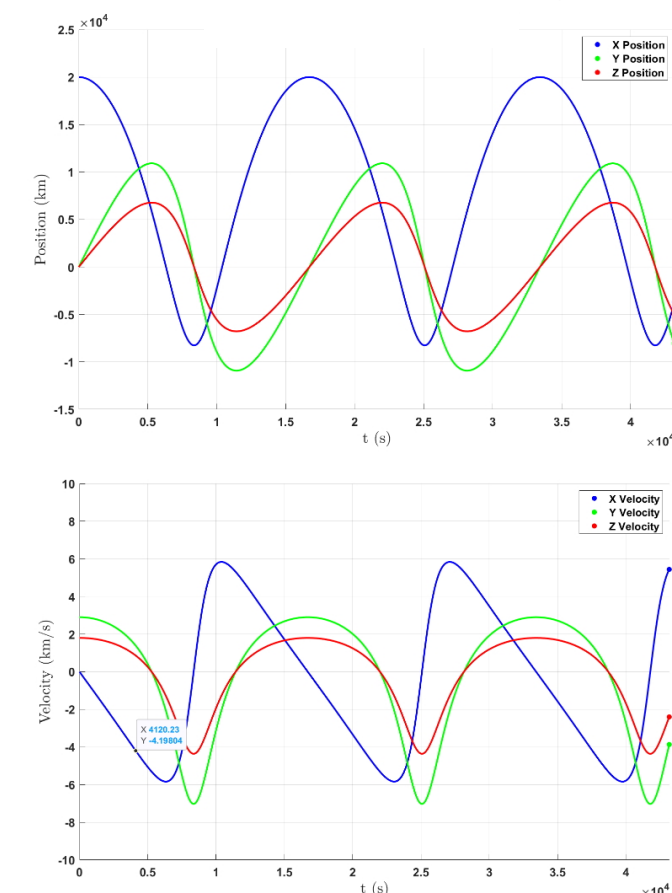
- Accuracy and efficiency results of GBEES compared to MC simulations in regimes where it is expected that the EKF may fail are promising, but require more tweaking if we are to feasibly argue it can compete computationally

- Rigorous computational profile may determine where bottlenecks are occurring
- Complete examination of conditions where EKF fail may also be beneficial for demonstrating regimes/mission trajectories of interest



- Next step will be representing and propagating uncertainty in a higher-fidelity, six-dimensional system

- A jump in dimensionality means an increase in computational burden
- This may be alleviated by time-marching in a variable set that changes slower (orbital elements)





This investigation was partially supported by the NASA Space Technology Graduate Research Opportunity (Grant Number 80NSSC23K1219)

All code can be found at: <https://github.com/bhanson10/GBEES>

Thank you for your time. Questions?